Exploring quality inspection and grade judgment of distortion defects in the fabrication of spectacle lenses

Hong-Dar Lin[a], Tung-Hsin Lee[a], Chou-Hsien Lin[b] and Yuan-Shyi Peter Chiu[a*]

[a]Department of Industrial Engineering and Management, Chaoyang University of Technology, Taichung, Taiwan
[b]Department of Civil, Architectural, and Environmental Engineering, University of Texas at Austin, Austin, Texas, United States

CHRONICLE	ABSTRACT
	This study explores the quality control system featuring visual inspection and grade judgment for detecting distortion defects in spectacle lens fabrication. Spectacle lenses must be precisely curved to help accommodate nearsightedness and farsightedness. The curved shape allows the lens to have different curvatures in different areas during grinding. The spectacle lens will be prone to optical distortion when the curvature changes abnormally. Accordingly, this study proposes an automatic distortion flaw inspection system for spectacle lenses to substitute professional inspectors who rely on empirical judgment. We first apply the digital imaging of a concentric circle pattern through a testing lens to create an image of that lens. Second, the centroid–radii model is employed to stand for the shape property of each concentric circle in the image. Third, by finding the deviations of the centroid radii for detecting distortion flaws through a small variation control method, we obtain a different image showing the detected distortion regions. Four, based on the distortion amounts and locations, we establish the fuzzy membership functions and inference rulesets to measure distortion severity. Finally, the GA-ANFIS model is applied to determine the quality levels of distortion severity for the detected distortion flaws. Trial outcomes reveal that the proposed automatic inspection system can help practitioners in spectacle lens fabrication, for it attains a high 94% correct classification rate of quality grades in distortion severity, 81.09% distortion flaw detection rate, and 10.94% fake alert rate, in distortion inspection of spectacle lenses.

1. Introduction

The increased dependence and burden on the eyes have led to a gradual increase in the demand for eyeglasses to assist vision. Spectacle lenses are curved to accommodate nearsightedness and farsightedness. The curved shape allows the lens to have different curvatures in different areas within the lens during grinding. The spectacle lens is made by grinding the transparent lens to bend the lens, mainly through the slight change of the curvature, so that the lens power can meet the needs of the user. However, the spectacle lens will be prone to optical distortion during imaging when the curvature changes abnormally.

In the process of lens manufacturing, due to the different curvatures of each area, the difficulty of grinding the lens is much higher than that of ordinary lenses. Often, the negligence of the manufacturer can easily cause distortion flaws that are very serious for users. Since the lenses are directly used to cover the eyes, the distortion flaw of the lens will lead to imaging errors bringing inconvenience and even danger to the user in daily life activities. Figure 1 shows the schematic illustrations of imaging distortion for viewing distant street scenes with the normal and defective spectacle lenses, respectively.

<center>(a)   (b)</center>

Fig. 1. Schematic illustrations of imaging distortion for viewing distant street scenes with spectacle lenses: (a) normal lens, (b) defective lens

Distortions occurring in the near central part need to be paid attention to because these distortions will directly affect the imaging quality of the user's viewing of objects. For example, when going downstairs, you may experience dizziness or be unable to accurately judge the position between steps, which may be dangerous to people. Currently, the degree of distortion in this area is checked manually with the aid of an instrument. If the distortion is too severe, it needs to be regarded as defective, otherwise, it will endanger the life of the wearer. The current testing instruments only measure the lens data such as the power and transmittance of the lens. There is no instrument to quantify and detect distortion flaws and only relies on the experience and judgment of professionals. Therefore, the lens manufacturing industry urgently needs a set of automatic distortion inspection systems with consistency, accuracy, and cycle detection advantages.

If wearing lenses with severe imaging distortion flaws, consumers will see distorted scenes and may encounter inconvenience or even danger in daily life activities. Since imaging distortions do not have regular shapes and sharp boundaries, they are often difficult to detect and measure, especially on curved spectacle lenses. In addition, outwardly curved lenses, due to their high light transmittance and high reflectivity, often hinder the identification of distortion flaws in spectacle lenses. This study proposes an automated vision system for rapid detection and classification of distortion flaws to replace the use of high-end optical instruments and personnel when inspecting lenses during manufacturing, resulting in cost savings and improved overall inspection efficiency and effectiveness.

2. Literature Reviews

Automatic optical inspection in quality evaluation has become an essential process for production as it ensures that product quality is assured and production efficiency is enhanced through strict inspection and evaluation of all products in the industrial processes (Ebayyeh & Mousavi, 2020; Chen et al., 2021). The inspection systems established on image processing and machine learning technology have generated many appliances in the manufacturing industry (Tulbure, 2022). To improve glass product qualities, many studies have been developing non-contact automatic inspection devices inspecting the shape and poor surface of a glass product with the latest image processing technologies, and analyzing the characteristics of glass. These researches investigated the surface defect inspection of glass-related products, such as proposing a multi-crisscross filtering method established on the Fourier domain to detect appearance blemishes of capacitive touch panels (Lin & Tsai, 2012), designing a visual inspection system for non-spherical lens modules of semiconductor sensors (Kuo et al., 2017), applying the Hotelling's T2 statistic and grey clustering methods to cosine transform for detection of visible defects in appearances of LED lenses (Chiu & Lin, 2013), designing an inspection structure for auto glass using fringe patterns (Xu et al., 2010). These optical inspection systems focus mainly on surface flaw detection on glass-related products.

Image distortions because of perspective have to be corrected to permit further image processing (Daniel et al., 2017). Regarding the distortion detection and correction techniques, Mantel et al. (2020) proposed methods for determining the perspective distortion on electroluminescence images of photovoltaic panels, and Cutolo et al. (2020) presented a quick method to calibrate transparent head-mounted panels by making the use of a calibrated camera. It is evident that most of the distortion-related works due to perspective concentrate on the distortion correction of optical lenses (Hou et al., 2018; Liu et al., 2018).

Transmitted deformation is the image degeneration of a visible object incurred by transpicuous materials. In inspection studies of transmitted distortion in industrial parts, Dixon et al. (2011) developed a system using digital imaging and a classifier based on decision trees for quantifying optical distortion in aircraft transparencies. Youngquist et al. (2015) presented a novel explanation of optical distortion and permitted the use of a phase-shifting interferometer for determining the distortion of a large optical window. Lin and Hsieh (2018) designed a vision system with a trapezoidal mask for image acquisition and applied small shift control charts to inspect distortion flaws on car mirrors. Gerton et al. (2019) investigated distortion patterns of Ronchi grids mathematically for determining the effects of distortions in eyewear products. Lin and Lo (2016) applied Hough transform to detect distortion defects on transparent glass products.

Spectacle lenses are products that are closely related to people's activities and must be verified in the inspection. If there are too many defects, it will lead to dangers in people's lives. Le et al. (2019) used symmetric energy analysis of color channels to automatically detect surface defects for coated eyeglasses. Yao et al. (2013) applied forward lighting by low-angled-ring-LED for image capture and normalization algorithms for image processing and glasses grading to develop a surface defect inspection system for glasses. Karangwa et al. (2021) proposed an optical inspection platform combining convolutional neural networks and semantic segmentation to inspect and classify appearance flaws on optical plane components, such as lenses, filters, mirrors, etc. Lin et al. (2019) proposed a visual inspection system for optical components based on computer vision, widely applied in the flaw inspection of lenses for cameras and eyeglasses and other optical elements. Lin (2014) proposed an adaptive vision-based approach that combines the extraction of wavelet features and a support vector machine classifier for classifying various classes of spectacle lens images to judge the power of spectacle lenses.

Most current optical inspection systems for transparent glass products mainly detect surface defects but do not include imaging distortion flaws. The imaging distortion flaws embedded in the surface of curved spectacle lenses with high transmission and reflection characteristics are difficult to detect accurately (Lin and Hsieh, 2018). Most of the related works on perspective-induced distortion have focused on the distortion correction of optical lenses. Presently, very few research studies apply automated visual inspection systems to detecting imaging distortion flaws in eyeglass lenses. Therefore, we propose a vision system based on small variation control methods to inspect imaging distortion flaws on spectacle lenses. With proper parameter settings, the method can identify not only severe distortion flaws but also minor distortion ones.

3. Proposed approach based on the small variation control method

This study proposes a vision-based system with a known standard pattern for image acquisition and applies small variation control methods to inspect distortion flaws as well as a hybrid intelligent model of combining genetic algorithm and fuzzy inference system to determine the quality level of distortion severity on curved spectacle lenses. To measure the distortion degree of a curved spectacle lens, we first apply the digital imaging of the concentric circles pattern through a testing lens to create an imaging distortion map of that lens. This distortion map is regarded as an imaging image to be analyzed to find the existence of distortions and locations of the flaws. Second, the imaging image is preprocessed to increase the appearance clearness of the concentric circles and the distance features between the mass center and boundary points of each concentric circle based on a centroid-radii model are extracted for shape descriptions in the image. Third, through the small variation control method to find slight changes in the distance deviations in the features for detecting distortion flaws, a different image displaying the detected distortion flaws can be obtained. Four, based on the distortion amounts and occurrence locations in the training stage, the fuzzy membership functions and inference rulesets of the distortions are established. Finally, the GA-ANFIS model is applied to classify the quality levels of distortion severity for the detected distortion flaws.

3.1 Image acquisition and Preprocessing

In this study, testing samples with a 6.3 mm thickness and a 49.6 mm diameter, are randomly selected from the fabrication line of a spectacle lens manufacturer. To acquire images with digital imaging of a standard pattern through a testing sample for creating an imaging distortion map of the sample, this study proposes an image capture system with a concentric circles pattern for imaging image acquisition. Fig. 2 shows a testing lens sample and two transmitted imaging images using the concentric circles pattern for image acquisition. The testing sample is inserted in a custom-made fixture horizontally and is located in front of the standard pattern. The standard pattern with base concentric circles is attached to the bottom. A camera with a stand is used to take images from the view transmitted on the concentric circles pattern through the testing lens. To acquire the digital imaging of a standard pattern with proper intensity, the lighting control of the environment is also important when acquiring images.

Fig. 2. A testing lens sample and two acquired imaging images using the concentric circles pattern for image acquisition

Fig. 3 shows two processed images from transmitted imaging of the concentric circles pattern through a defective lens. The defective image has significant distortions in the lower-left area. The captured images are preprocessed in some steps to increase the clearness of object appearances on transpicuous lenses. To quantify the distortion level of the captured pattern image, Figure 3(a) and Figure 3(b) depict the corresponding binarized image and thinned image for the defective sample

that the Otsu method (Otsu, 1979) and thinning algorithm (Zhang & Suen, 1984) are applied to do segmentation and thinning operation sequentially while using the concentric circles pattern. Most of the concentric circles are segmented and thinned from the background in the binary thinned images by the two methods. The results disclose that the moderate distortion faults in transpicuous lens surfaces are rightly divided in the binary images, irrespective of insignificant distortion differences.
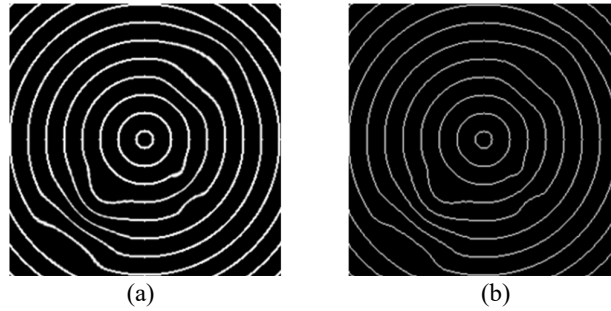

(a) (b)

Fig. 3. Two processed images from transmitted imaging of the concentric circles pattern through a defective lens: (a) the binarized image; (b) the thinned image

3.2 Feature extraction of distortion flaws

Some problems arise when using coordinates directly for image feature processing. If the image is translated, scaled, and rotated, the result of feature judgment will be wrong due to the change of coordinates. Therefore, it needs to be described by geometric features. In this study, the centroid–radii model (Tan et al., 2000) is employed to stand for the geometric property of each concentric circle in the image, and the coordinates are converted into distance feature vectors through Euclidean distance. Euclidean distance has the properties: translation invariance, scaling invariance, and rotation invariance.

A typical concentric circles pattern includes 8 concentric circles in this study. The centroid radii d_i^m are the Euclidean distances calculated from the centroid $C(x_c, y_c)$ and the i-th boundary point $(x_{i,m}, y_{i,m})$ on the m-th circle of the concentric circles pattern, correspondingly:

$$d_i^m = \sqrt{(x_{i,m} - x_{c,m})^2 + (y_{i,m} - y_{c,m})^2}$$ (1)

The centroid radii of the m-th circle in the concentric circles pattern can form a distance-vector denoted as,

$$D_m = \{d_1^m, d_2^m, d_3^m, ..., d_i^m, ...\}$$ (2)

The distance vector can be further normalized to between 0 and 1 for scale and rotation invariance by dividing the maximum value of the distance values,

$$N_i^m = d_i^m / \max(d_i^m)$$ (3)

When the centroid radii from the concentric circles to the object centroid are calculated and normalized, Fig. 4(a) draws the schematic diagram of the distance feature vector of all points of a concentric circle. Fig. 4(b) shows the farther the distance feature is from the middle, the more this area is represented for concentric circles there are potential distortions.
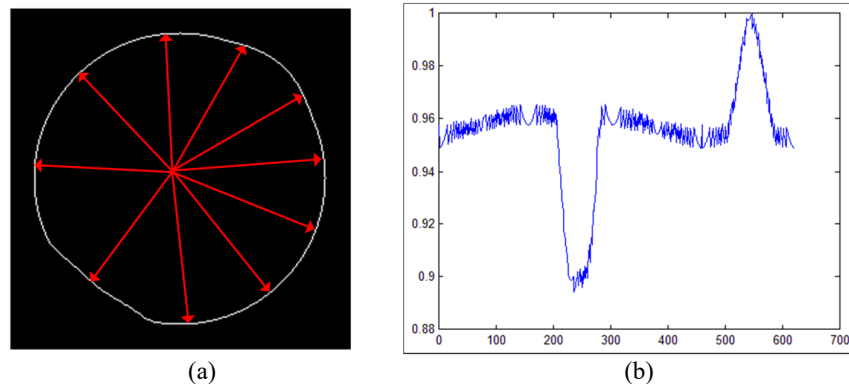

(a) (b)

Fig. 4. The corresponding distance values from the mass center to the boundary points of a concentric circle: (a) the

schematic diagram of the Euclidean distances (b) the boundary points versus the normalized distance values.

3.3 Distortion detection by the EWMA method

The feature values of the concentric circles pattern in the testing image are compared with those of the normal image to measure the deviation of the corresponding distances to locate suspicious distortions in the testing image. To detect small changes in distance deviation, this study proposes one of the small variation control techniques, the EWMA (exponentially weighted moving average) method, which is often applied in statistical process control to detect slight deviations or shifts from the normal production process (Montgomery, 2019; Mansouri et al., 2018). We apply this method to find slight changes in the distance deviations for detecting distortion flaws. The EWMA method is a good choice for detecting slight deviations in process control of industrial applications (Sanusi et al., 2017; Mitra et al., 2019). The exponentially weighted moving average Z_i is expressed as:

$$Z_i = \lambda x_i + (1-\lambda)Z_{i-1} \tag{4}$$

where λ is a constant on an interval $0<\lambda \leq 1$ and the start value of Z_i is the process target value $Z_0=\mu_0$. Values of the parameter λ called smoothing constant or weight in the interval 0.05 ~ 0.25 are suitable in practice for small deviation detection. A suggested regulation is to use a litter value of λ to detect slight deviations. A lower bound and an upper bound for the control limits (LCL and UCL) of the EWMA method are calculated as:

$$UCL_i = \overline{X} + L\sigma\sqrt{\frac{\lambda}{2-\lambda}\left[1-(1-\lambda^{2i})\right]} \tag{5}$$

$$LCL_i = \overline{X} - L\sigma\sqrt{\frac{\lambda}{2-\lambda}\left[1-(1-\lambda^{2i})\right]} \tag{6}$$

The planned parameters of the chart are the multiple of the standard deviation employed in the bound limits (L) and the value of λ. The manifestation of the EWMA method is simple to establish and manipulate. Fig. 5 shows the detection result of the 7-th circle of the concentric circles pattern in the sample image processed by the EWMA method. It can be seen that when the EWMA detects regions with distortion flaws, there will be clearer boundary point ranges for the locations of the flaws.
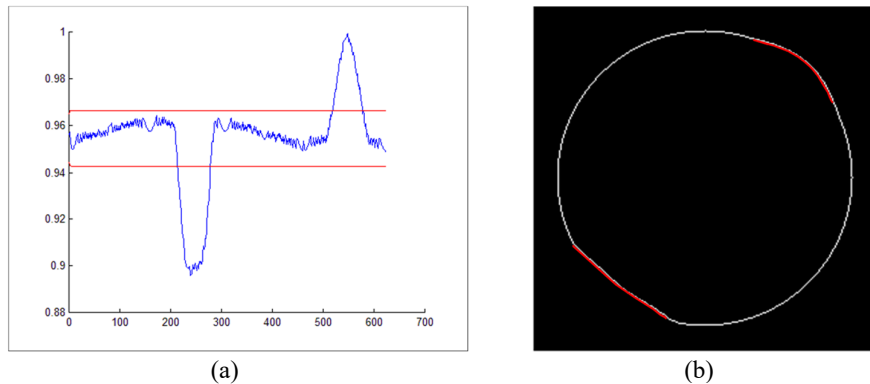

(a) (b)

Fig. 5. The detection result of the 7-th circle of the concentric circles pattern in the sample image processed by the EWMA method: (a) the EWMA control chart; (b) the regions of detected distortion flaws marked in red

3.4 Determination of quality grades for distortion severity by GA-ANFIS method

This study uses fuzzy measurement models for automatic variation detection of distortion severity (Vahid et al., 2018). The GA-ANFIS (Genetic Algorithm-Adaptive Network-based Fuzzy Inference System) is a system combining genetic algorithm and adaptive network fuzzy inference system theory, including GA and ANFIS, of which ANFIS includes FIS and BPN (Back-Propagation Network). The GA-ANFIS model is employed to classify the quality level of the distortion severity of spectacle lenses. By combining the advantages of these algorithms, the classification accuracy of the system is significantly improved. By comparing the differences between the detected distortion flaw image and the concentric circles pattern image, Fig. 6(a) displays the red-line areas are the distortion flaws and the white-line areas are the standard pattern. And, the detected flaw points are compared with the points on the concentric circles pattern, correspondingly. The Manhattan distance-vector M representing the amount of distortion is calculated as:

$$m_j = \left|x_{d,\,j} - x_{p,\,j}\right| + \left|y_{d,\,j} - y_{p,\,j}\right|, \tag{7}$$
$$M = \{m_1, m_2, m_3, \ldots, m_j, \ldots\}, \tag{8}$$

where $x_{d,j}$ and $y_{d,j}$ are the coordinates of the j-th point on the distorted image, and $x_{p,j}$ and $y_{p,j}$ are the coordinates of the j-th point on the concentric circles pattern.
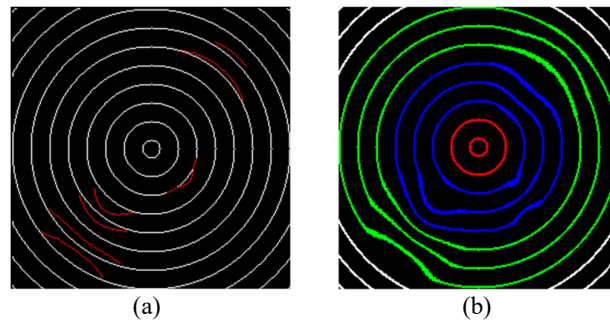

<div align="center">(a)   (b)</div>

Fig. 6. The processed distortion images are (a) the difference image with marked distortions, and (b) the marked difference image based on three different severity levels of distortion

Fig. 6(b) shows that the marked difference image is divided into three areas based on three different severity levels of distortion: the red part is the low-tolerance region, which consists of the 1st and 2nd circles, called area A; the blue part is the medium-tolerance region, which is composed of the 3rd, 4th, and 5th circles, called area B; the green part is the high-tolerance region, which is made up of the 6th, 7th, and 8th circles, called area C. The individual distortion measures of these three areas are input into the inference system for inference and classification.

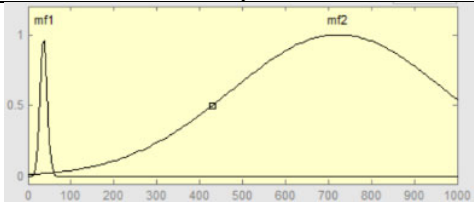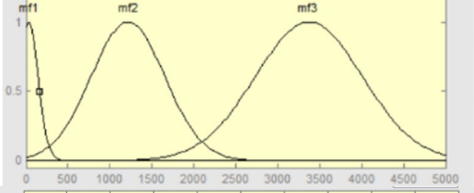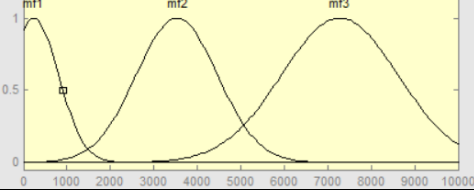*3.4.1 FIS of distortion severity*

The principal function of the fuzzy inference system (FIS) is to convert the observations into fuzzy membership functions and to establish fuzzy inference rules and models (Shihabudheen & Pillai, 2018; Takagi & Sugeno, 1985). The advantage is that when the input is fuzzy data, it can output a suitable corresponding value through the process of conducting the established inference rules and a de-fuzzy algorithm. In this study, the amounts of distortion in areas A, B, and C are used as inputs to classify the severity levels of lens distortions. Table 1 lists three feature values as the inputs of the fuzzy inference system, which are the individual levels of distortion amounts in areas A, B, and C, and the output value is the distortion severity. In the level setting of the fuzzy sets, when the input value is the distortion amount in area A, it is set to 2 levels due to the low tolerance, and the rest of the input and output values are all 3 levels. All membership functions and fuzzy sets for the inputs are computed and summarized in Table 2.

Table 1
The inputs and outputs of the proposed fuzzy inference system

	Inputs			Outputs
Feature values	X_1: Distortion amount in area A	X_2: Distortion amount in area B	X_3: Distortion amount in area C	Y: Deformation severity
Levels	A_1: Small A_2: Large	B_1: Small B_2: Medium B_3: Large	C_1: Small C_2: Medium C_3: Large	O_1: Minor O_2: Moderate O_3: Severe

After the fuzzy membership functions are established, the fuzzy rule base can be formulated according to the tolerance of the distortion degree of the spectacle lens. When the area where the distortion defect occurs is closer to the center of the lens, the allowable tolerance is smaller, and the distortion severity is at a serious level. The closer the distortion defect area is to the boundary of the lens, the higher the allowable tolerance and is therefore classified as minor on the distortion severity scale. We formulate fuzzy rules based on the empirical rules of professionals. There are three input values: X_1, X_2, and X_3, which are the levels of distortion amounts in areas A, B, and C, and the output value is the severity level. For example, when the distortion amount (X_1) in area A is small (A_1) and the distortion amount (X_2) in area B is small (B_1) and the distortion amount (X_3) in area C is small (C_1), the output severity level (Y) is minor distortion (O_1). A fuzzy rule base including 18 rules is established in this study. The inference engine employed in this study is the TSK (Takagi-Sugeno-Kang) fuzzy model (Takagi & Sugeno, 1985) combining the use of fuzzy rules with the IF-THEN form. The outcome of every rule is a linear association of the input variables and a constant item. The resulting outcome is the weighted mean of every rule outcome. It mainly uses fuzzy rules to depict a nonlinear system. The advantages of this method are fast calculation efficiency, better coordination with adaptive optimization technology, and continuous surface values in outputs. These are great for mathematical analysis. When the levels of distortion amounts of the three areas are input into the fuzzy inference system and inferred by all the rules, a correct output value can be generated through the defuzzification process using the weighted average method. After calculating the output values of all rules, the final output value can be obtained.

Table 2
The membership functions and fuzzy sets for the inputs

Inputs	Membership functions	Fuzzy sets
Distortion amount X_1 in area A		$\mu_{A_1}(x;\ 8.26, 4.784)$ $\mu_{A_2}(x;\ 1084, 765)$
Distortion amount X_2 in area B		$\mu_{B_1}(x;\ 69, 17.61)$ $\mu_{B_2}(x;\ 385, 895.7)$ $\mu_{B_3}(x;\ 384, 2392)$
Distortion amount X_3 in area C		$\mu_{C_1}(x; 287, 117.2)$ $\mu_{C_2}(x; 468.5, 1766)$ $\mu_{C_3}(x; 670, 3637)$

3.4.2 ANFIS for judging the severity of distortions

ANFIS is mainly a network inference model established by combining the two principles of backward propagation neural network and fuzzy inference system (Jang, 1993; Karaboga & Kaya, 2018). It is evaluated by continuously changing parameter values and minimizing the error function. In this study, a five-layer ANFIS network architecture diagram is established through the distortion amounts of the three areas, which are the input layer, rule layer, normalization layer, result inference layer, and output layer, as shown in Fig. 7. Through a learning process, training is performed iteratively, and each training will repeatedly correct the parameters and calculate the error values of the parameters. When the training error value converges to the minimum value or the training reaches the set maximum number of learning times, the training will be stopped, and a better network fuzzy inference system can be obtained than the original parameters.
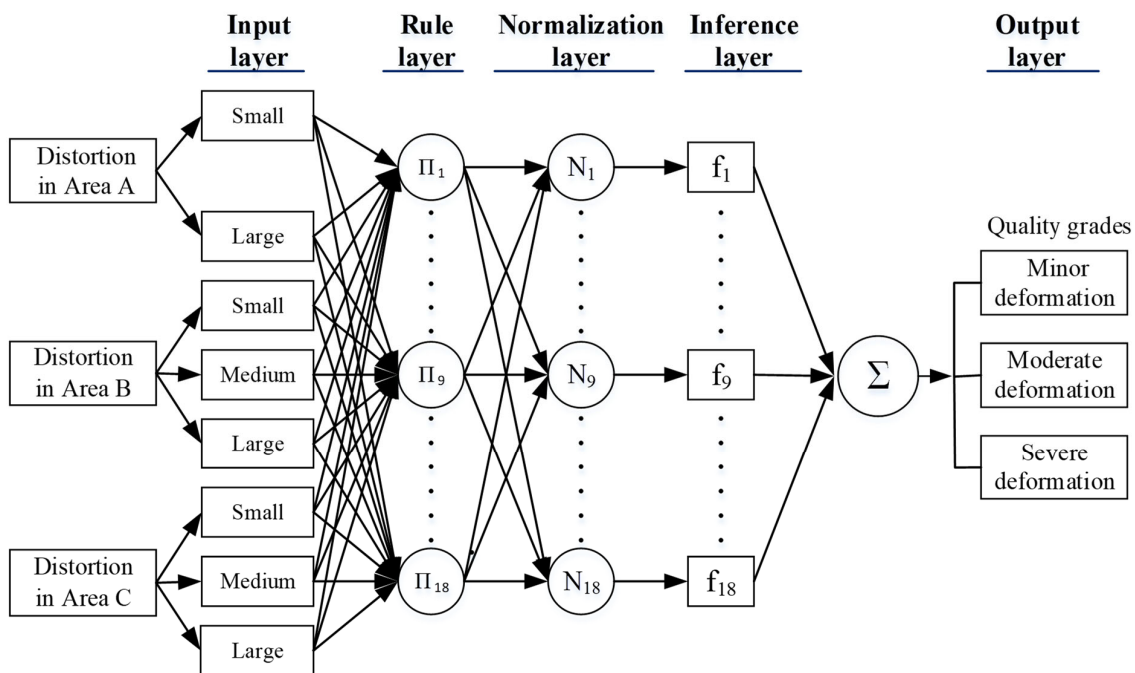
Fig. 7. The proposed ANFIS structure diagram for judging the severity of distortions

3.4.3 GA-ANFIS for classifying severity levels of distortions

The Genetic Algorithm (GA) mainly applies the process of biological reproduction and inheritance through crossover and mutation of chromosomes. First, use the parameters of the membership function of the distortion amount to establish the initial population of the genetic algorithm, and assess the fit value of every parameter combination in the population. Next, the parameters in each parameter combination perform uniform crossover and mutation to generate more different parameter values. The advantage of this algorithm is that it can be promoted to the global optimal solution from the local optimal one through the mutation function. A fuzzy inference system has been established including the membership functions of the distortions in three regions, the rule base and the inference mode. The GA-ANFIS model mainly optimizes the algorithm through two steps (Li & Su, 2010; Vishal et al., 2019). The first step of optimization is to use the ANFIS to compute the errors between the predicted solutions and the ground-truth values and the solution is optimized by a gradient descent method. But using the gradient descent method can only find the local optimal solution. The second step of optimization is to use the GA to evaluate the fitness values of the parameter combinations and select better parameters from crossover to share information, and finally, perform mutation to make the range of feasible parameters wider. The purpose of this step is to promote the local optimal solution to the global optimal solution.

4. Implementation and Analyses

To evaluate the manifestation of the recommended method with the concentric circles pattern, assessments are performed on 350 sample images (200 images for training and 150 images for testing) with various severity levels of distortions to evaluate the capability of the recommended technique. Every captured image has 256x256 pixels with 8 bits per pixel. The developed distortion flaw inspection arithmetic is compiled in the Matlab platform and carried out on the version R2013 of MATLAB interactive environment on a computer (INTEL CORE i5-8250U 1.60GHz, 16GB RAM). To numerically verify the capability of the distortion flaw inspection methods, we discern the results of our assessments from those offered by the empirical evaluators (gold standard). Two measures, (1-α) and (1-β), are employed to indicate suitable detection appraisals; the greater the two measures, the more correct the examination consequences. Fake alert error α, considering regular regions as distortion flaws, divides the districts of regular regions inspected as distortion flaws by the districts of detected results as distortion regions to acquire the error. Losing alert error β, defeating to alert true distortion flaws, divides the districts of undetected true distortion flaws by the districts of overall true distortion flaws to gain the error.

4.1 Detection results of using the concentric circles pattern with various line thicknesses

The pixel size of line thickness in the concentric circles image will affect the detection performance of distortion flaws by the proposed method. If a suitable pixel size of line thickness is selected in the concentric circles image, the smaller distortion flaws will be more completely identified. We examine the concentric circles pattern with 1 to 6-pixel sizes of line thicknesses in the concentric circles images by the proposed method. Figure 8 shows the captured and resulting images for the defective sample by the proposed method using the concentric circles pattern with the six-pixel sizes of line thicknesses, respectively. We find that the smallest pixel thickness is less sensitive to the detection of distortion flaws and causes the lowest detection rate. In addition, the larger pixel thicknesses are more sensitive to the detection of distortion flaws and cause more fake alert errors. Table 3 indicates the detection results using the 2 and 3-pixel sizes of line thicknesses for the concentric circles pattern is suitable and has better distortion inspection performance because of the higher detection rate and lower fake alert rate.
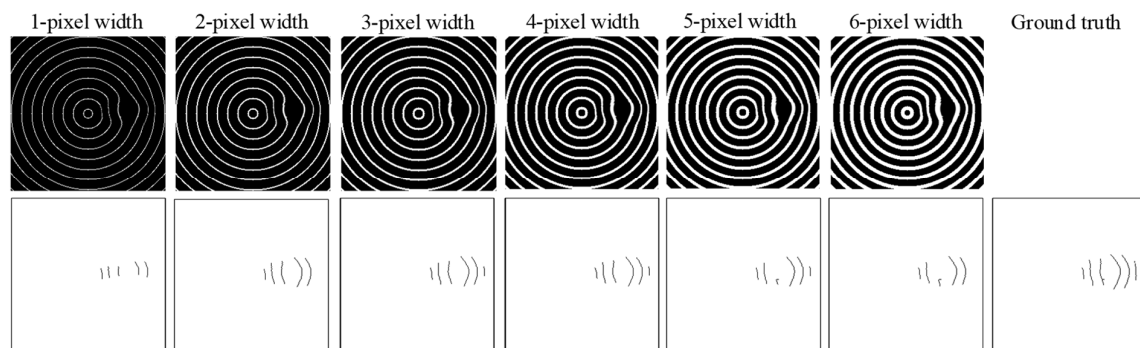

Fig. 8. The defective captured images and their corresponding resulting images of distortion flaw inspection by the proposed method for producing the concentric circles with various line thicknesses.

Table 3
Performance indices of distortion flaw inspection by the proposed method for captured images using the concentric circles pattern with various line thicknesses

Line thicknesses	1-pixel	2-pixel	3-pixel	4-pixel	5-pixel	6-pixel
Fake alert rate (α)	0.0507	0.0398	0.0398	0.0953	0.0468	0.0894
Detection rate (1-β)	0.5436	0.8072	0.8012	0.7590	0.7915	0.7749

4.2 Detection results of using various small variation control methods by the proposed method

To assess the performance of the distortion flaw inspection on spectacle lenses, Table 4 summarizes the inspection results of the proposed method in this study. Two small variation control methods, the MA (Moving Average) (Montgomery, 2019) method and the EWMA method, of the proposed approach are assessed against the outcomes by empirical evaluators. The average distortion detection rates (1-β) of whole test trials by the two schemes are 66.18% (MA method) and 81.09% (EWMA method). Nevertheless, the MA method has a significantly larger fake alert rate (α), 56.51%. Otherwise, the EWMA method has a fairly smaller fake alert rate, 10.94%. The suggested EWMA method has a larger distortion inspection rate and a smaller fake alert rate than does the MA method applied to distortion flaw detection on curved spectacle lenses. Figure 9 demonstrates the fractional results of imaging distortion inspection by the proposed approach using two distinct small variation control methods. The average execution time for processing a testing image is as below: 0.3045 sec. by the MA method and 0.3249 sec. by the EWMA method. The mean conducting time of the two schemes is nearly the same. Hence, the suggested EWMA method conquers difficulties of detecting distortion flaws on spectacle lenses and surpasses its ability to accurately differentiate slight distortion flaws from regular regions.

Table 4
Performance indices of distortion inspection by the proposed method for detecting distortion regions and determining quality levels on spectacle lenses.

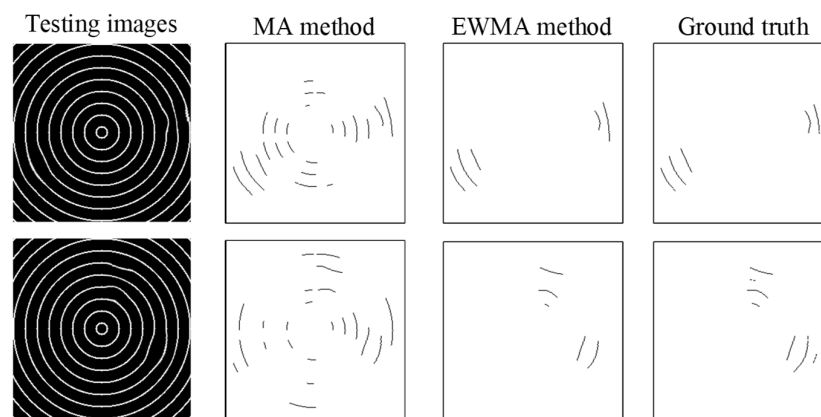| Distortion inspection methods	MA method		EWMA method	
Fake alert rate (α)	0.5651		0.1094	
Detection rate (1-β)	0.6618		0.8109	
Processing time (Sec.)	0.3045		0.3249	
Severity classification methods	ANFIS	GA-ANFIS	ANFIS	GA-ANFIS
Correct classification rate (CR)	0.6467	0.8067	0.7067	0.9404

Fig. 9. Partial results of imaging distortion inspection by the proposed method using two distinct small variation control methods.

To evaluate the performance of classifying the severity of distortion flaws on spectacle lenses, two classification models, ANFIS and GA-ANIFS, are also assessed against the outcomes by professional inspectors. From Table 4, no matter which distortion inspection method is used, the correct classification rate of distortion severity by the GA-ANFIS model is higher than that of the ANFIS model. From the above analyses, we conclude that the proposed hybrid approach of combining the EWMA method and GA-ANFIS model is a better detection and classification method for imaging distortion inspection and

quality level determination on spectacle lenses.

4.3 Comparisons of distortion detection results by the existing methods and the proposed approach using different standard patterns

Two common standard patterns, checkers pattern and dots pattern, were used to detect distortions by the Lin and Lo approach (2016) for differentiating outcomes of distortion flaw inspection. Since we use the three standard patterns to produce consistent images of distortion flaws by selecting the same distortion areas and the same degrees of distortions, the distortion differences among the three standard patterns can be compared more accurately. To reveal the distortion inspection effects of the consistent captured images, Fig. 10 illustrates partial results of inspecting distortion flaws by the Lin and Lo method and the proposed method using the checkers pattern, dots pattern, and concentric circles pattern, and the gold standard (ground truth) supplied by empirical evaluators, separately.
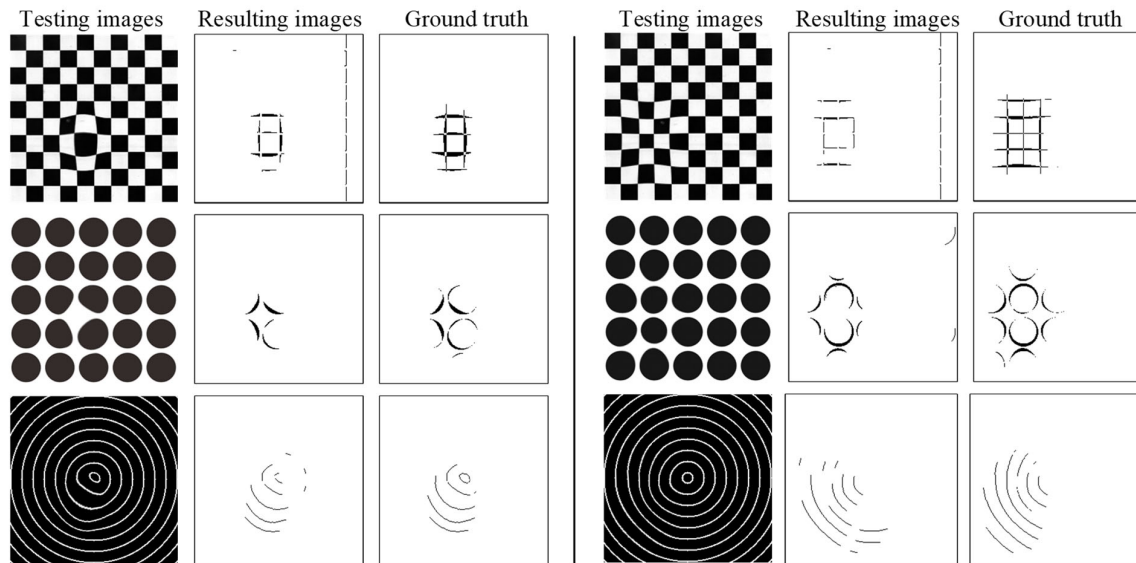

Fig. 10. Partial results of imaging distortion inspection by the Lin and Lo method and the proposed method using three common standard patterns

The Lin and Lo method using the checkers pattern produces many incorrect discernments not only in losing alerts but also in fake alerts, and the same approach using the dots pattern also causes some of the incorrect discernments in losing alerts and fake alerts on distortion flaw inspection of spectacle lenses. The proposed method using the concentric circles pattern inspects most of the distortion flaws and produces fewer incorrect discernments. Table 5 summarizes the detection outcomes of imaging distortion inspection by the Lin and Lo method and the proposed method using the three standard patterns. It indicates that the proposed method using the concentric circles pattern is superior to the existing methods with the checkers pattern and dots pattern in the distortion flaw inspection on spectacle lens images.

Table 5
Performance indices of imaging distortion inspection by the Lin and Lo method and the proposed method using three common standard patterns

Standard patterns	Fake alert rate	Detection rate	Correct classification rate
Checkers pattern	0.6236	0.3324	0.9470
Dots pattern	0.1878	0.5820	0.9894
Concentric circles pattern	0.2314	0.7703	0.9947

5.   Concluding Remarks

This study attempts to find a way to substitute the human evaluators in the fabrication process by developing a hybrid approach established on computer vision and machine learning to inspect distortion flaws and determine quality levels on spectacle lenses. This research investigates the detection of imaging distortion flaws and the classification of distortion severity in spectacle lens images. We first developed a vision system using the concentric circles' pattern to capture testing images displaying imaging distortion regions. Next, the concentric circle edges in the image are binarized and thinned. If

the distances from the boundary points of the concentric circles to the centroid exceed the control limits of the proposed EWMA method, it indicates the presence of distortion flaws. Then, we compare the detected flaw image with the standard pattern and calculate the number of distortions. By dividing the possible flaw locations into three areas A, B, and C, we summarize the individual distortion amounts in these three areas. Finally, the GA-ANFIS model is proposed to classify the levels of distortion severity on spectacle lenses. The proposed method effectively detects distortion flaws and classifies the severity of distortion regions on spectacle lens images. Trial outcomes reveal the proposed approach attains a high 94% correct classification rate of quality levels in distortion severity, 81.09% distortion flaw detection rate, and 10.94% fake alert rate, in distortion inspection of spectacle lenses. Further research can expand the suggested approach to the defect detection problems of imaging distortion of similar products, such as deformation inspection of transparent glass and deformation detections of mirror products.

Acknowledgments

References

Abu Ebayyeh, A.M., & Mousavi, A. (2020). A review and analysis of automatic optical inspection and quality monitoring methods in electronic industry. *IEEE Access*, *8,* 183192-183271.

Chen, Y., Ding, Y., Zhao, F., Zhang, E., Wu, Z., & Shao, L. (2021). Surface defect detection methods for industrial products: a review. *Applied Sciences*, *11*(16), 7657.

Chiu, Y.-S. P., & Lin, H.-D. (2013). An innovative blemish detection system for curved LED lenses. *Expert Systems with Applications*, *40*(2), 471-479.

Cutolo, F., Fontana, U., Cattari, N., & Ferrari, V. (2020). Off-line camera-based calibration for optical see-through head-mounted displays. *Applied Sciences*, *10*(193), 1-19.

Daniel, S.C., Luis, G., Miguel, A.F., Agustin, S., Julio, E., Luis, M., & Luis, A. (2017). Automatic correction of perspective and optical distortions. *Computer Vision and Image Understanding*, *161*, 1-10.

Dixon, M., Glaubius, R., Freeman, P., Pless, R., Gleason, M.P., Thomas, M.M., & Smart, W. (2011). Measuring optical distortion in aircraft transparencies: a fully automated system for quantitative evaluation. *Machine Vision and Applications*, *22*(5), 791-804.

Gerton, K.M., Novar, B.J., Brockmeier, W., & Putnam, C. (2019). A novel method for optical distortion quantification. *Optometry and Vision Science*, *96*(2), 117-123.

Hou, Y., Zhang, H., Zhao, J., Jian, H., Hao, Q., Liu, Z., & Guo, B. (2018). Camera lens distortion evaluation and correction technique based on a colour CCD moiré method. *Optics and Lasers in Engineering*, *110*, 211-219.

Jang, J.S.R. (1993). ANFIS: Adaptive-Network-based Fuzzy Inference Systems. *IEEE Transactions on Systems, Man, and Cybernetics*, *23*(3), 665-685.

Karangwa, J., Kong, L.H., Yi, D.R., & Zheng, J.S. (2021). Automatic optical inspection platform for real-time surface defects detection on plane optical components based on semantic segmentation. *Applied Optics*, *60*(19), 5496-5506.

Karaboga, D., & Kaya, E. (2018). Adaptive network-based fuzzy inference system (ANFIS) training approaches: a comprehensive survey. *Artificial Intelligence Review*, *52*(4), 2263-2293.

Kuo, C.-F. J., Lo, W.-C., Huang, Y.-R., Tsai, H.-Y., Lee, C.-L., & Wu, H.-C. (2017). Automated defect inspection system for CMOS image sensor with micro multi-layer non-spherical lens module. *Journal of Manufacturing Systems*, *45*, 248-259.

Le, N.T., Wang, J.-W., Wang, C.-C., & Nguyen, T.N. (2019). Automatic defect inspection for coated eyeglass based on symmetrized energy analysis of color channels. *Symmetry*, *11*, 1518.

Li, K., & Su, H. (2010). Forecasting building energy consumption with hybrid genetic algorithm-hierarchical adaptive network-based fuzzy inference system. *Energy and Buildings*, *42*, 2070-2076.

Lin, H.-D., & Tsai, H.-H. (2012). Automated quality inspection of surface defects on touch panels. *Journal of the Chinese Institute of Industrial Engineers*, *29*(5), 291-302.

Lin, H.-D., & Lo, Y.-C. (2016). Automated distortion defect inspection of transparent glass using computer vision. *Proceedings of the 2016 International Conference on Image Processing, Computer Vision, and Pattern Recognition*, 235-240.

Lin, H.-D., & Hsieh, K.-S. (2018). Detection of surface variations on curved mirrors of vehicles using slight deviation control techniques. *International Journal of Innovative Computing, Information and Control*, *14*(4), 1407-1421.

Lin, T.-K (2014). An adaptive vision-based method for automated inspection in manufacturing. *Advances in Mechanical Engineering*, ID: 616341, 1-7.

Lin, Y., Xiang, Y., Lin, Y., & Yu, J. (2019). Defect detection system for optical element surface based on machine vision. in: *2019 IEEE 2nd International Conference on Information Systems and Computer Aided Education*, 415-418.

Liu, S., Li, Z., Zhong, K., Chao, Y.J., Miraldo, P., & Shi, Y. (2018). Generic distortion model for metrology under optical microscopes. *Optics and Lasers in Engineering*, *103*, 119-126.

Mansouri, M., Harkat, M.F., Nounou, M., & Nounou, H. (2018). Midpoint-radii principal component analysis -based EWMA and application to air quality monitoring network. *Chemometrics and Intelligent Laboratory Systems*, *175*, 55-64.

Mantel, C., Villebro, F., Parikh, H.R., Spataru, S., dos Reis Benatto, G.A., Sera, D., Poulsen, P.B., & Forchhammer, S. (2020). Method for estimation and correction of perspective distortion of electroluminescence images of photovoltaic panels. *IEEE Journal of Photovoltaics*, *10*(6), 1797-1802.

Mitra, A., Lee, K.B., & Chakraborti, S. (2019). An adaptive exponentially weighted moving average-type control chart to monitor the process mean. *European Journal of Operational Research*, *279*(3), 902-911.

Montgomery, D.C. (2019). *Introduction to Statistical Quality Control*, 8th Edition, John Wiley & Sons, New York, NY, USA.

Otsu, N. (1979). A threshold selection method from gray level histogram. *IEEE Transactions on Systems, Man and Cybernetics*, *9*, 62-66.

Sanusi, R.A., Riaz, M., Adegoke, N.A., & Xie, M. (2017). An EWMA monitoring scheme with a single auxiliary variable for industrial processes. *Computers & Industrial Engineering*, *114*, 1-10.

Shihabudheen, K.V., & Pillai, G.N. (2018). Recent advances in neuro-fuzzy system: A survey. *Knowledge-Based Systems*, *152*, 136-162.

Takagi, T., & Sugeno, M. (1985). Fuzzy identification of systems and its applications to modeling and control. *IEEE Transactions on Systems, Man, and Cybernetics*, *15*(1) 116-132.

Tan, K.L., Ooi, B.C., & Thiang, L.F. (2000). Indexing shapes in image databases using the centroid-radii model. *Data & Knowledge Engineering*, *32*, 271-289.

Tulbure, A.-A., Tulbure, A.-A., & Dulf, E.-H. (2022). A review on modern defect detection models using DCNNs-Deep convolutional neural networks. *Journal of Advanced Research*, *35*, 33-48.

Vahid, S., Farshid, F.A., & Hamid, E. (2018). A new fuzzy measurement approach for automatic change detection using remotely sensed images. *Measurement*, *127*, 1-14.

Vishal, K., Ashwani, K., Deepak, C., & Pratyoosh, S. (2019). Improved biobleaching of mixed hardwood pulp and process optimization using novel GA-ANN and GA-ANFIS hybrid statistical tools. *Bioresource Technology*, *271*, 274-282.

Xu, J., Xi, N., Zhang, C., Shi, Q., & Gregory, J. (2010). A geometry and optical property inspection system for automotive glass based on fringe patterns. *Optica Applicata*, *40*(4), 827-841.

Yao, H.B., Ping, J., Ma, G.D., Li, L.W., & Gu, J.N. (2013). The system research on automatic defect detection of glasses. *Applied Mechanics and Materials*, *437*, 362-365.

Youngquist, R.C., Skow, M., & Nurgle, M.A. (2015). Optical distortion evaluation in large area windows using interferometry. in: *14th International Symposium on Nondestructive Characterization of Materials*, Marina Del Rey, California, USA.

Zhang, T.Y., Suen, C.Y. (1984). A fast parallel algorithm for thinning digital patterns. *Communications of the ACM*, *27*(3), 236-239.